Capturing the Stratosphere's Influence on Seasonal and Intraseasonal Predictability in a State-of-the-Art Navy Global Environmental Model (NAVGEM)

Stephen D. Eckermann
Geospace Science & Technology Branch
Code 7631, Space Science Division
Naval Research Laboratory
Washington DC 20375
Phone: (202) 404-1299   Fax: (202) 404-7997   email: stephen.eckermann@nrl.navy.mil

LONG-TERM GOALS

Recent research has revealed that the stratosphere influences medium- and long-range weather prediction, sometimes strongly (NAS 2010). The North Atlantic Oscillation (NAO) – one of the most prominent modes of intraseasonal tropospheric variability extending from the subtropical Atlantic to the Arctic (Hurrell et al. 2003) – has been recognized only within the past decade as one regional manifestation of a larger hemispheric phenomenon, known synonymously as the Arctic Oscillation (AO) or Northern Annular Mode (NAM). The NAM extends continuously into the stratosphere and mesosphere, and an analogous deep Southern Annular Mode (SAM) occurs in the southern hemisphere. NAM/SAM anomalies often appear first in the upper stratosphere or mesosphere, then descend gradually over a period of weeks, sometimes reaching the surface where they change weather patterns throughout the polar region (Baldwin and Dunkerton 2001; Coy et al. 2011). Descending stratospheric NAM/SAM anomalies also play a pivotal role in controlling the response of high-latitude weather to the El-Niño/Southern Oscillation in the tropics (Bell et al. 2009; Ineson and Scaife 2009), while the tropical stratosphere and mesosphere may also impact tropical seasonal prediction through an improved Madden-Julian Oscillation (Weare et al. 2012). These examples, and others like them, point to the important role that the overlying stratosphere-mesosphere system can play in presaging and regulating large-scale global surface weather changes over periods of weeks to months (e.g., Baldwin et al. 2003), prompting recent reports from the World Climate Research Programme (WCRP 2008) and the National Academy of Sciences (NAS 2010) that note (quote) "*the stratosphere's potential to improve seasonal forecasts is largely untapped.*"

Thus the long-term goals of this project are to tap the potential of an improved stratosphere and mesosphere for seasonal prediction by developing and testing new stratospheric and mesospheric modeling, prediction and data assimilation capabilities, all specifically designed to improve long-range prediction capabilities of the Navy Environmental Global Model (NAVGEM).

		Form Approved OMB No. 0704-0188

Report Documentation Page

1. REPORT DATE **2012**	2. REPORT TYPE **N/A**	3. DATES COVERED **-**

4. TITLE AND SUBTITLE	5a. CONTRACT NUMBER
Capturing the Stratospheres Influence on Seasonal and Intraseasonal Predictability in a State-of-the-Art Navy Global Environmental Model (NAVGEM)	5b. GRANT NUMBER
	5c. PROGRAM ELEMENT NUMBER
6. AUTHOR(S)	5d. PROJECT NUMBER
	5e. TASK NUMBER
	5f. WORK UNIT NUMBER
7. PERFORMING ORGANIZATION NAME(S) AND ADDRESS(ES) **Geospace Science & Technology Branch Code 7631, Space Science Division Naval Research Laboratory Washington DC 20375**	8. PERFORMING ORGANIZATION REPORT NUMBER
9. SPONSORING/MONITORING AGENCY NAME(S) AND ADDRESS(ES)	10. SPONSOR/MONITOR'S ACRONYM(S)
	11. SPONSOR/MONITOR'S REPORT NUMBER(S)

12. DISTRIBUTION/AVAILABILITY STATEMENT
Approved for public release, distribution unlimited

13. SUPPLEMENTARY NOTES
The original document contains color images.

14. ABSTRACT

15. SUBJECT TERMS

16. SECURITY CLASSIFICATION OF:			17. LIMITATION OF ABSTRACT	18. NUMBER OF PAGES	19a. NAME OF RESPONSIBLE PERSON
a. REPORT **unclassified**	b. ABSTRACT **unclassified**	c. THIS PAGE **unclassified**	**SAR**	**15**	

Standard Form 298 (Rev. 8-98)
Prescribed by ANSI Std Z39-18

OBJECTIVES

The overarching objective of this proposal is to gain an improved understanding of how the stratosphere and mesosphere in a state-of-the-art numerical weather prediction (NWP) system affect atmospheric prediction on time scales from days to months. To achieve this, our research focuses on the following scientific questions:

1. What are the fundamental dynamics and dominant physical coupling pathways governing the stratosphere-troposphere interaction that are most relevant for atmospheric prediction on time scales from days to months?

2. Which physical and dynamical processes in the forecast model are important in controlling this deep vertical coupling, and how sensitive is forecast skill to details in their numerical implementation?

APPROACH

Our primary tool is NAVGEM, the Navy's next-generation NWP system, comprising a new semi-Lagrangian (SL) global forecast model coupled to the four-dimensional variational (4DVAR) NRL Atmospheric Variational Data Assimilation System – Accelerated Representor (NAVDAS-AR). Our approach to utilizing NAVGEM for this research is guided by the following recommendations of WCRP (2008) and NAS (2010) to address knowledge gaps in our current understanding of coupled troposphere-stratosphere predictability:

R1. Models *must* extend to *at least* 0.01 hPa (~80 km altitude) with a full range of appropriate physical parameterizations, so as to properly predict stratospheric and mesospheric variability;

R2. Research should then focus on the extended system's ability to reproduce and delineate the poorly understood connections between stratospheric and tropospheric circulations.

R1 Tasks

To address R1, our project is progressively augmenting the NAVGEM SL forecast model and DAS in ways that improve its ability to predict the integrated troposphere-stratosphere-mesosphere system, as outlined in tasks (a)-(e) below. These tasks are described, justified and linked scientifically in detail in the original science proposal.

(a) SL model tests using additional vertical layers and resolution

(b) Improved radiative heating and cooling rates for the SL model's stratosphere and mesosphere

(c) Improved ozone photochemisty for the upper stratosphere and mesosphere

(d) Parameterizations of subgrid-scale gravity-wave drag for the stratosphere and mesosphere

(e) Assimilation of stratospheric and mesospheric satellite observations

R2 Tasks

To address R2, we perform the following component tasks using the augmented NAVGEM model, as progressively developed via successful execution of the R1 tasks listed above. Again, these tasks are described and scientifically motivated in significant detail in the original science proposal.

(a)   Bias identification and parameterization correction/improvement

(b)   Forecast-assimilation experiments supporting international research projects on predictability

(c)   Realistic tropical QBO (quasi-biennial oscillation) and SAO (semiannual oscillation)

(d)   Prediction of stratospheric sudden warmings (SSWs) and stratospheric NAM/SAM anomalies

(e)   Tropospheric influences of stratospheric NAM/SAM anomalies

(f)   Tropospheric coupling to the stratospheric QBO

WORK COMPLETED

Task R1a. (<u>leads</u>: Steve Eckermann, Jim Ridout). Figure 1 summarizes three new vertical level formulations for NAVGEM that were developed this year and compares them to previous and existing formulations, both at FNMOC and at other centers. We developed and refined a new 50-level (L50) formulation (red curves) that replaced the previous L42 (black curves). This was chosen to improve resolution in the boundary layer and lower stratosphere, to aid a new SL model vertical mixing parameterization and assimilation of new infrared nadir radiance channels, respectively. After a series of beneficial test experiments, the L50 formulation transitioned to the NAVGEM "trunk" (main code repository) yielding a T359L50 NAVGEM configuration as the version extensively tested for inaugural transitioning to operations at FNMOC, planned to occur in late 2012. To extend NAVGEM above the current upper boundary of 0.04 hPa (~65 km), we also generated two new candidate formulations also shown in Figure 1: an L64 scheme (orange curves) extending to 0.00566 hPa (~85 km) and an L71 scheme (gray curves) extending to 0.000766 hPa (~99 km). These schemes were chosen to match the tropospheric and lower stratospheric thicknesses of the new preoperational L50 scheme (see Figure 1a), then to transition to constant thicknesses of ~2 km throughout the stratosphere and mesosphere (see Figure 1b). These levels were built into developmental versions of NAVGEM and are currently being tested.

Task R1b. (<u>leads</u>: Steve Eckermann, Jim Ridout, Code 7500) With colleagues at NRL Monterey, this year the previous narrowband Harshvardhan (1987) parameterizations were replaced in NAVGEM with the multiband rapid radiative transfer model for GCM applications (RRTMG) parameterizations based on the Atmospheric Environment Research Ltd. (AER) radiative transfer codes of Mlawer et al. (1997) and Clough et al. (2005). In single column tests, we showed that the new RRTMG schemes give excellent results up to ~0.1 hPa (~65 km), higher than the older schemes, and give stable results to higher altitudes. However, errors may grow in the mesosphere due to missing physics, such as the effects of breakdown of the local thermodynamic equilibrium (LTE) assumption for the radiative transfer of both 15 μm and near-IR bands of the dominant CO_2 emissions above ~70 km altitude. These issues are being investigated further in single column experiments.
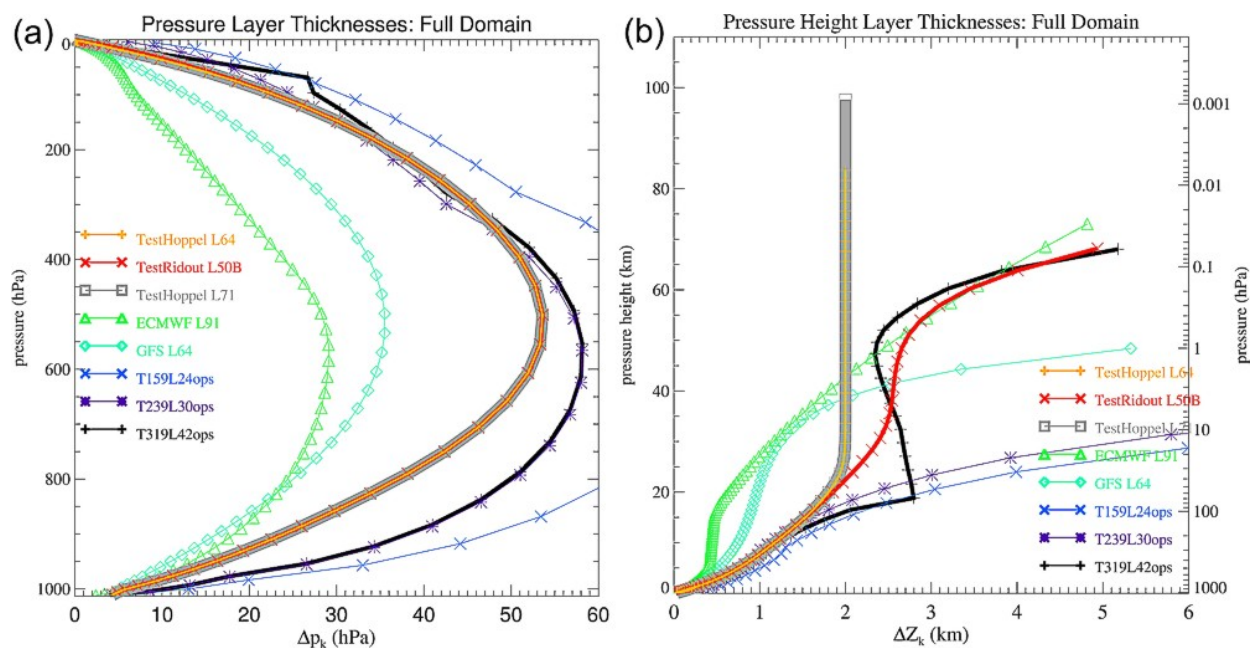
Figure 1. NAVGEM vertical model levels, plotted (a) as pressure thicknesses versus pressure (hPa) and (b) as pressure height thicknesses versus pressure height (km). Plots show previous NOGAPS 24-level (L24) and 30-level (L30) formulations (blue and purple, respectively), earlier NOGAPS and NAVGEM L42 (black), and the current operational configurations of the NCEP GFS (L64: aqua) and ECMWF IFS (L91: green). Our new L50 NAVGEM formulation is plotted in red extending to ~70 km, which replaced to previous L42 formulation. High-altitude L64 and L71 formulations with improved ~2 km resolution throughout the stratosphere and mesosphere are plotted in orange and gray. See text for further details.
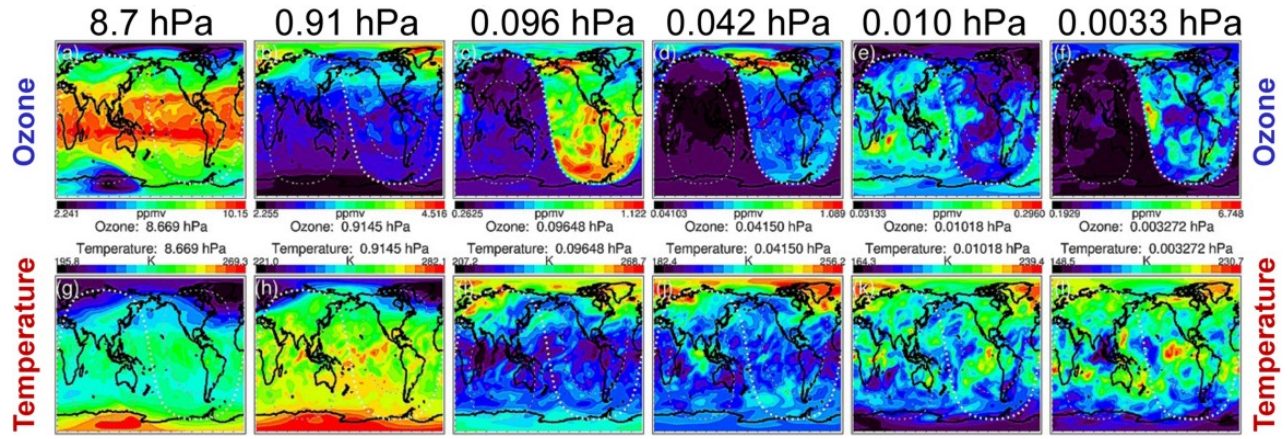
Figure 2. Global maps of ozone volume mixing ratio (ppmv, top row) and temperature (bottom row) from a +54 hour hindcast initialized on 1 November 2007 at 0000 UTC. These instantaneous (unaveraged) model fields are plotted with increasing altitude, progressing from left to right, of 8.7 hPa, 0.91 hPa, 0.096 hPa, 0.042 hPa, 0.010 hPa, and 0.0033 hPa. The solar terminator (cosχ=0) is plotted as the white dotted curve, and the cosχ=±0.5 contours are plotted as gray dotted curves (after Eckermann and McCormack 2012).

Task R1c. (leads: Steve Eckermann, John McCormack) Significant progress was made in extending the current diurnal-mean NRL linearized ozone photochemistry parameterization of McCormack et al. (2006) to accurately model large day-night asymmetries in ozone mixing ratio that develop above ~50 km. The photochemical basis of the new scheme is involved and currently being written up for potential publication in the peer-reviewed scientific literature (Eckermann and McCormack 2012), so only a brief summary is provided here. We have generalized atmospheric odd oxygen chemistry to include a height dependent partition ratio of monatomic oxygen to ozone concentrations, $\Lambda=[O]/[O_3]$, that tracks the transition from the stratosphere, where ozone is the major odd oxygen constituent, to the mesosphere and lower thermosphere (MLT) where O dominates. This leads to Λ-dependent perturbations to the diurnal mean linearized photochemical coefficients that increase with height. These are then scaled by a new gridpoint parameter ε_d, representing the fraction of the day that is sunlit (specified for efficiency using a seasonally varying global lookup table), which acts to convert the previous McCormack et al. (2006) diurnal-mean ozone photochemical coefficients into daytime values. We next include an entirely new nighttime photochemistry, which is very slow (essentially tracerlike) in the stratosphere but becomes progressively faster and hence more important at higher altitudes. This nighttime chemistry, based on the equilibrium recombination model of Allen et al. (1984), requires the addition of a new vertical profile of the ozone night-to-day ratio taken from a detailed offline photochemistry calculation. Finally, these separate daytime and nighttime photchemical coefficients must be carefully combined across the terminator using a zenith-angle dependent interpolation, along with a localized photochemical rate increase to mimic rapid chemical recombination just after sunset. The new scheme was extensively tested in a new global offline NAVGEM simulator. This extension from single column to global proved necessary here to test and remove some early issues with the zenith-angle dependence of the new chemistry near the terminator.

The scheme was implemented initially in the NOGAPS-ALPHA forecast model and a nature run was performed starting on 1 November 2007 and extending for ~20 days. Figure 2 plots global maps of prognostic ozone mixing ratios (top row) and temperatures (bottom row) at t=+54 hours at progressively increasing altitudes, beginning at 9 hPa (left column), where there is little detectable day-night ozone asymmetry, and ending at 0.003 hPa (right column), where realistic large day-night asymmetries are evident across the solar terminator in the simulations arising from the new diurnal chemistry. Visual inspection of the maps at higher altitudes reveals clear, geophysically-realistic ozone-temperature anticorrelations. This work continues with planned implementation of the new scheme in the NAVGEM SL model as part of a generalized ozone photochemistry code that can easily switch between a variety of schemes, including the old diurnal-mean chemistry of McCormack et al. (2006) and the new diurnal chemistry.
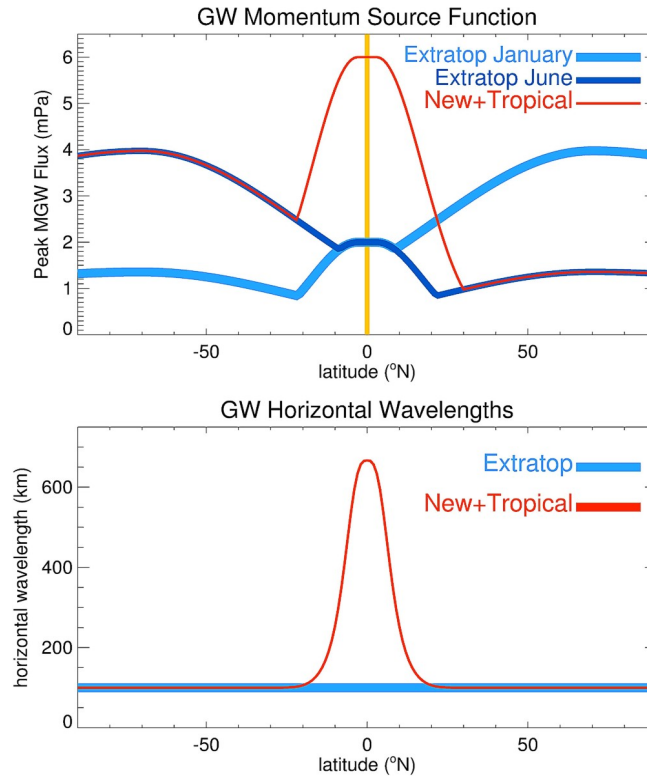

Figure 3. Plots of the wave source spectra for (top) total wave momentum (mPa) and (b) horizontal wavelength (km) as implemented this year in the stochastic gravity-wave drag parameterization of Eckermann (2011). Extratropical settings are shown in blue/purple, tropical settings in red.

Task R1d. (leads: John McCormack, Karl Hoppel) Our new single-wave stochastic parameterization of nonorographic gravity-wave drag (Eckermann 2011) was extended to include new separate source parameterizations relevant for the tropics and extratropics. In particular, as depicted in Figure 3, we added to the tropics a new source of wave momentum with long horizontal wavelengths to capture the equatorially trapped long wavelength modes that arise here with significant energy due to vanishing of the Coriolis parameter and forcing from deep tropical convection. These settings were tuned in long-term nature runs to generate tropical circulations described in Task R2c below. The scheme was subsequently implemented and tuned in NAVGEM (see Task R2a below) for data assimilation experiments described below under Task R1e.
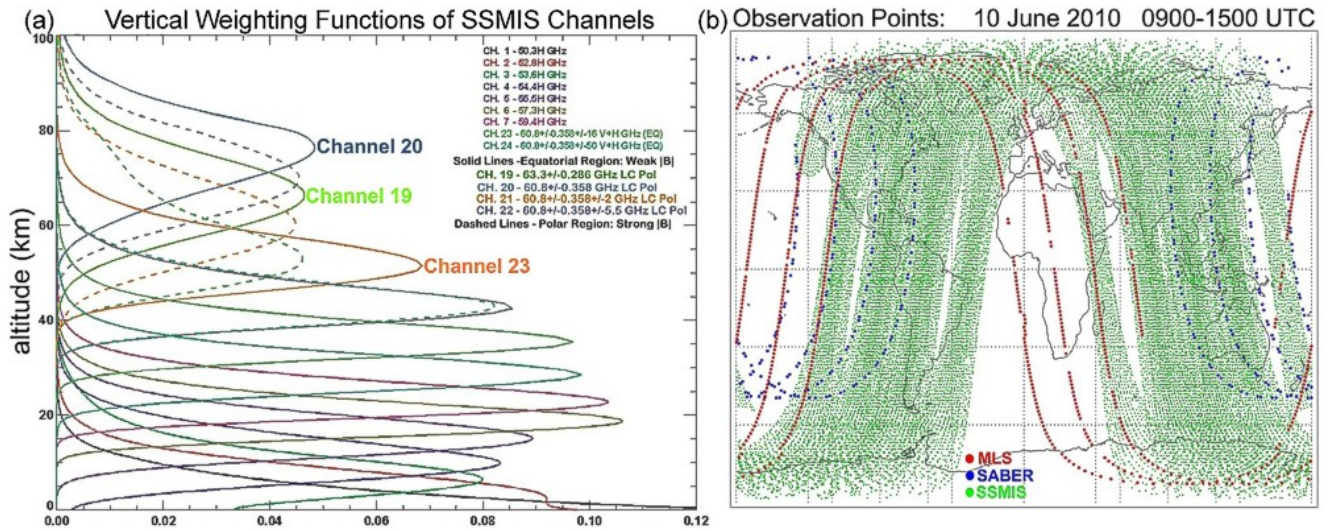
Figure 4. (a) SSMIS vertical weighting functions for a weak geomagnetic field typical of equatorial regions (solid curves) and for a strong magnetic field typical of polar regions leading to Zeeman splitting of the O₂ microwave lines (dashed curves). (b) MLT measurement locations for MLS (red), SABER (blue) and SSMIS on DMSP F16, F17 and F18 (green) on 10 June 2010 from 0900-1500 UTC.

Task R1e. (lead: Karl Hoppel): A high-altitude T239L60 NAVGEM was configured and parameterized gravity-wave drag was tuned for preliminary experiments to assimilate for the first time the 6 upper atmosphere sounding (UAS) thermal radiance channels of the Special Sensor Microwave Imager/Sounder (SSMIS) currently operating on the operational F16, F17 and F18 satellites of the Defense Meteorological Satellite Program (DMSP). Vertical contribution (weighting) functions (VWFs) for radiances acquired in a subset of the 24 SSMIS measurement channels are plotted in Figure 4a, revealing that these UAS channels acquire atmospheric temperature information up to ~100 km altitude. Since the 6 UAS channels use narrow spectral bands near line centers of the O_2 magnetic dipole transitions, then, as shown in Figure 4a, these channel radiances are significantly impacted by the Zeeman interaction of the O_2 molecule's electronic spin with the Earth's magnetic field, as well as by Doppler shifts due to the rotation of the Earth. Thus the key addition for accurately assimilating the temperature information contained in these radiances was integrating into NAVGEM the latest fast radiative transfer model of Han et al. (2007, 2010), which accounts for these physical processes in the assimilation using new geophysical inputs of the geomagnetic field vector and antenna pointing direction.
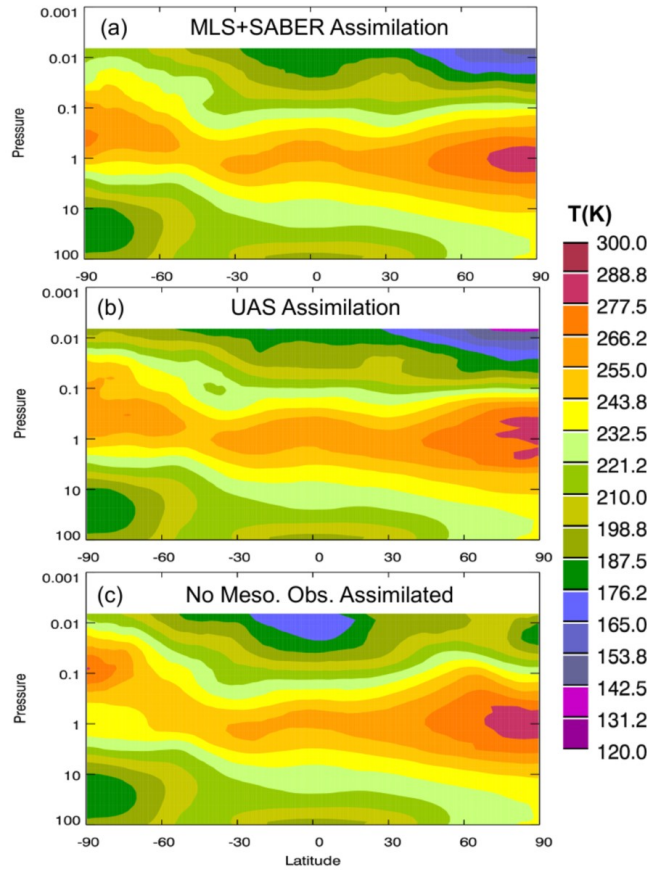
Figure 5. Zonal mean analyzed temperatures (K: see color bar) versus latitude and pressure from T239L60 NAVGEM experiments assimilating (a) MLS and SABER temperatures, (b) SSMIS UAS radiances and (c) no observations above ~ 1 hPa (after Hoppel et al. 2012).

Figure 5 plots zonal-mean analyzed temperatures from100-0.008 hPa on 14 July 2010 from a series of T239L60 NAVGEM forecast-assimilation experiments initialized on 20 June 2010. In all experiments the full complement of tropospheric and stratospheric observations from operational observing networks routinely assimilated by NOGAPS are used. Figure 5a shows results from an experiment that assimilated temperature profiles from two separate instruments on NASA research satellites: the Sounding of the Atmosphere Using Broadband Emission Radiometry (SABER) on NASA's TIMED satellite, and the Microwave Limb Sounder (MLS) on NASA's Aura satellite. Figure 4b plots typical sampling patterns of SABER and MLS mesospheric temperatures within a 6-hour analysis window. These observations extend through the stratosphere and mesosphere and were previously assimilated with the old 3DVAR NAVDAS using NOGAPS-ALPHA (Hoppel et al. 2008; Eckermann et al. 2009). Consistent with those earlier NOGAPS-ALPHA studies, this NAVGEM experiment produces a realistic mesospheric temperature analysis in Figure 5a, such as a cold summer mesopause at high northern latitudes and a separated (elevated) polar winter stratopause. Figure 5b shows corresponding results of assimilating SSMIS UAS radiances from F16, F17 and F18, but neither MLS nor SABER measurements: typical SSMIS observational sampling is also depicted in Figure 4b. Figure 5b reveals a very similar, accurate temperature analysis to Figure 5a, showing that assimilation of just these operational UAS channel radiances can provide an accurate mesospheric temperature analysis. To prove that this analysis skill is coming primarily from the assimilated observations and not from the

model, Figure 5c plots results from an experiment that assimilated no mesospheric observations. Here the mesospheric temperatures are significantly different to those in the panels above, indicating that the SL model still needs more physics tuning to remove mean temperature biases evident from this series of experiments. Indeed, this mesospheric data assimilation capability now allows model biases to be objectively diagnosed for the first time, providing bias and skill statistics that can now directly leverage Task R2a (bias identification and elimination) and other R1 tasks associated with mesospheric parameterization development. A publication on these results is being prepared for submission to the peer-reviewed scientific literature (Hoppel et al. 2012).

RESULTS

Task R2a. (leads: Karl Hoppel, Doug Allen, Steve Eckermann): This year the major work under this task focused on initial tuning of the new gravity-wave drag parameterizations (Task R1d) in NAVGEM to yield a reasonable mesosphere, so as to provide relatively unbiased temperature backgrounds for the assimilation of SSMIS UAS channels extending through the MLT (Task R1e). This has for the first time *objectively* identified upper-level SL model biases through forecast-assimilation experiments (c.f. Figures 5b and 5c). Figure 6 provides further objective data on biases associated with the standard deviations of the 3-9 hour forecasts with respect to objective observations, revealing enhanced standard deviations for the model forecasts without an MLT data assimilation constraints relative to those with. These new upper-level NAVGEM diagnostics in Figures 5-6 are now directly informing subsequent work focused on improving parameterizations of radiative and subgrid-scale dynamical driving of these upper-level regions in the SL model. Our work also identified the source of spurious tropical wind increment errors arising from the 4DVAR system, which were traced via offline experiments to meridional structure in upper-level tropical temperature increments, which were subsequently propagated into winds via the tangent-linear model (TLM) and adjoint. Work focused on removing this structured temperature bias (achieved primarily via a transition from Hermite to cubic vertical interpolation) has successfully suppressed these tropical wind increment errors, leading to improved tropical winds at all altitudes.
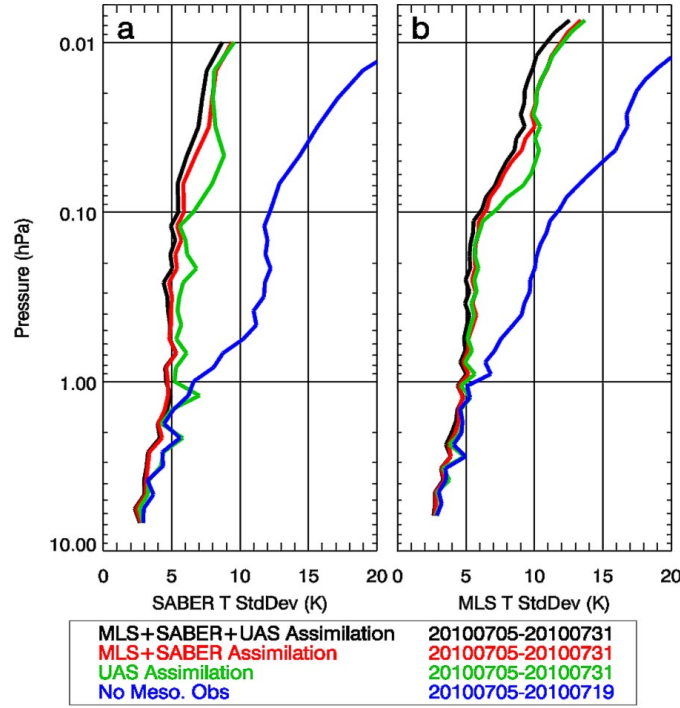
Figure 6. Standard deviation of observations minus forecasts for NAVGEM experiments assimilating no MLT observations (blue), SSMIS UAS radiances (green), SABER and MLS temperatures (red) and SABER, MLS and UAS observations (black). The observational comparisons use (a) SABER and (b) MLS temperatures (after Hoppel et al. 2012).
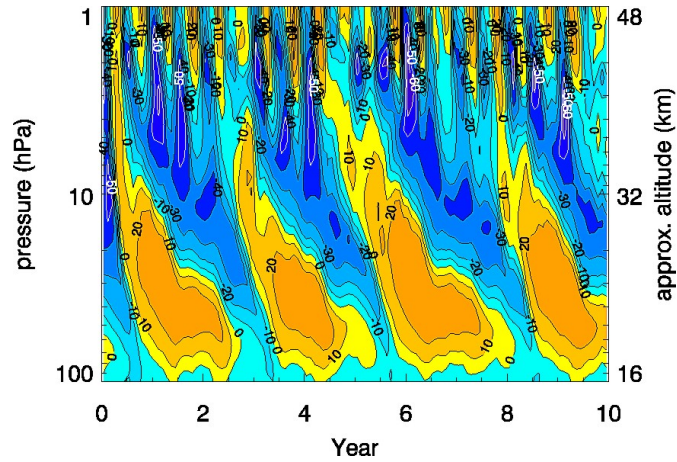

Figure 7. Mean zonal winds (m s^{-1}, red/yellow is eastward, blue is westward) from 5°S-5°N from a 7-year NOGAPS-ALPHA nature run at T79L139 using the Eckermann (2011) stochastic GWD parameterization with reduced vertical mixing and a new tropical wave source spectrum (results provided by J. P. McCormack 2012). Note the quasi-two-year wind oscillation in the lower stratosphere and the realistic SAO at higher altitudes.

Task R2b. (lead: Steve Eckermann): Our joint proposal for an international Stratospheric Network on Assessment of Predictability (SNAP) was selected by the World Climate Research Program for full requested support in August, with NRL one of 6 foundation members of the consortium from operational centers throughout the world (see http://www.sparcsnap.org/ for more details). SNAP will commence officially in January 2013, with a kickoff workshop in Reading in April 2013 where member centers (including NRL) will devise the pooled series of experiments they will conduct to support SNAP. At least one member of this project will attend and present at this kickoff workshop, after which the detailed experiments that support this task will commence.

Task R2c. (lead: John McCormack): Our new tropical source in the gravity-wave drag parameterization (Figure 3) was implemented in an effort to enable us to generate and maintain QBO and SAO circulations for the first time in Navy models. We performed a series of multi-year nature runs with NOGAPS-ALPHA as a means of refining parameter settings prior to implementing the capability in NAVGEM. A major breakthrough in maintaining these circulations in the model came from drastically (and realistically) reducing the amount of parameterized vertical mixing in the stratosphere, which was removing sharp QBO shear zones as they formed. Figure 7 shows tropical zonal-mean zonal winds from a 10-year T79L139 nature run with ~500 m vertical resolution in the stratosphere and mesosphere. For the first time in Navy models, we see in Figure 7 an internally generated and maintained zonal-wind QBO in the tropical lower stratosphere and zonal-wind SAO in the tropical upper stratosphere, which is now agreeing well with independent observations. This work will continue with efforts to transfer this new capability, which is critical for seasonal prediction, from the NOGAPS-ALPHA environment into NAVGEM.
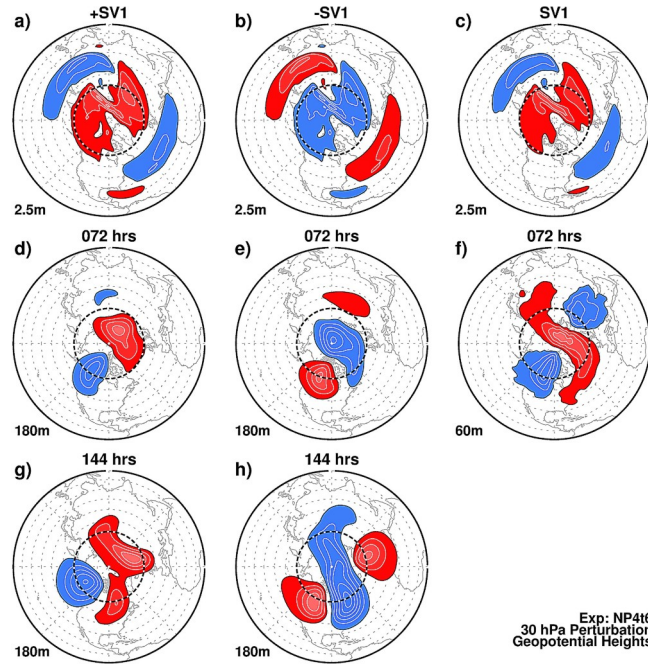

Figure 8. 30 hPa geopotential height perturbations from forecasts intialized by +SV1 perturbed (left column) and −SV1 perturbed (middle column) analyses, and NOGAPS SV system (right column) after 0 hours (top row), 72 hours (middle row) and 144 hours (bottom row). Positive (negative) perturbation anomalies are shaded red (blue) with white contours overlaid. Contour interval (meters) is given in lower left of each plot. Initial SV field in (c) is scaled to have same amplitude as selected for the forecast runs (a and b). The black and white dashed line marks 60°N.
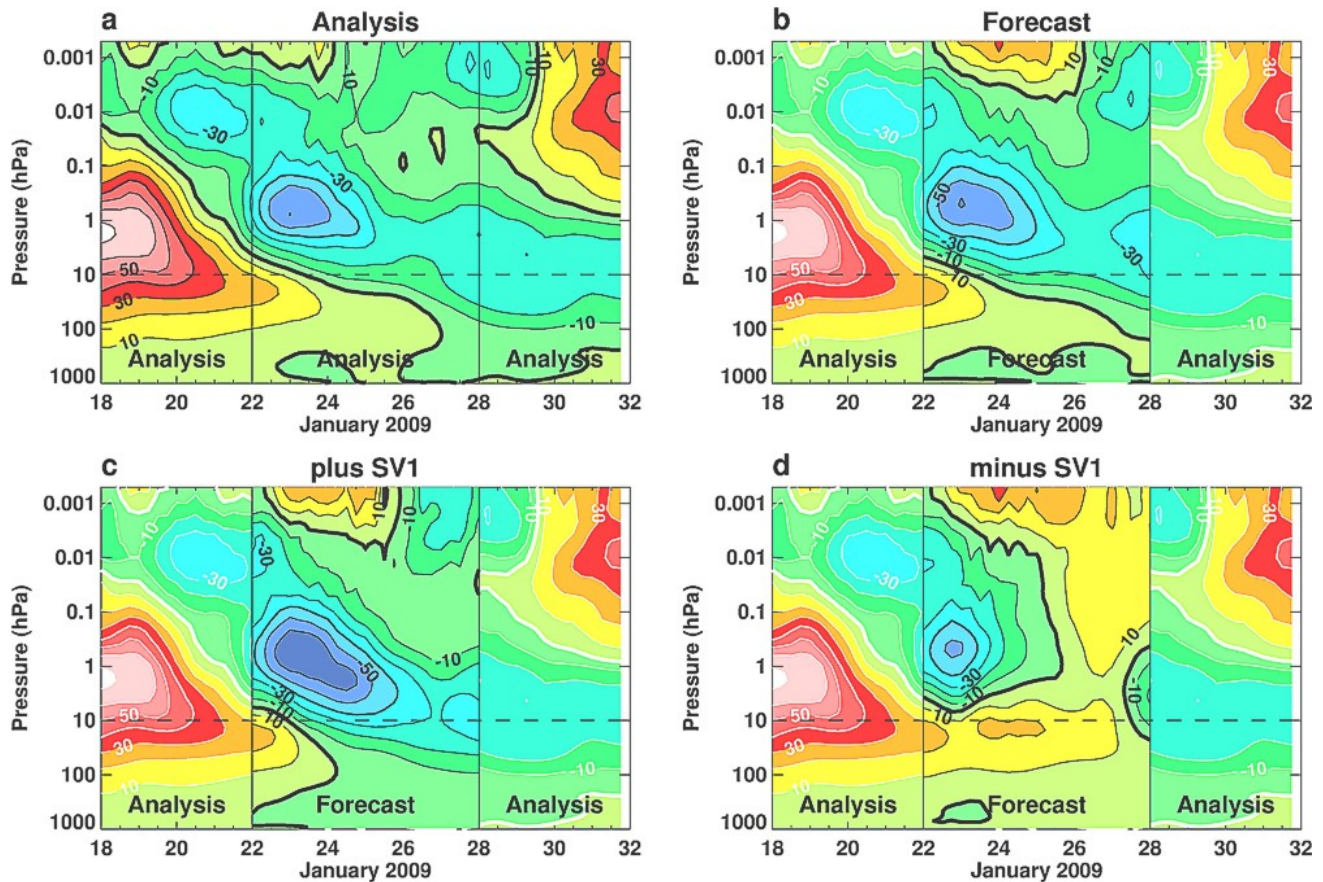
Figure 9. Time-height cross sections of zonal-mean zonal wind at 70°N (contour interval 10 m s⁻¹) for (a) NOGAPS-ALPHA analysis of Eckermann et al. (2009) from 18–31 January 2009. Remaining panels replace these analyzed winds from 22–28 January with winds from (b) control forecast, (c) +SV1 perturbed and (d) −SV1 perturbed forecasts.

Tasks R2d & R2e. (leads: Steve Eckermann, Carolyn Reynolds): We have made significant progress in diagnosing the role of evolving NAM/SAM anomalies during SSWs in controlling deep amospheric predictability through the use of stratospheric singular vectors (SVs) objectively diagnosed from the NOGAPS/NAVGEM TLM and adjoint. Top row of Figure 8 plots the leading singular vector (SV1) in forecasts for the period 22-25 January 2009 characterized by a record-breaking wave-2 major SSW. As opposed to earlier times when leading stratospheric SVs took the form of isolated tilted structures forming on vorticity gradients located at the extruded edges of the polar vortex, Figures 8a-c reveal that the stratospheric SV1 structure during the SSW takes on a completely different hemispheric annular structure that bears striking similarities to the climatological NAM. After 72 and 144 hours, remaining panels in Figure 8 reveal that the amplitude of this leading SV grows rapidly with time in both the high-altitude forecast model and in the NOGAPS SV system, while maintaining its hemispheric quasi-annular structure. The impact on SSW evolution and descending NAM anomalies is shown in Figure 9. Figure 9a plots the zonal-mean zonal winds during the 18-31 January 2009 period from the high-altitude NOGAPS-ALPHA analysis of Eckermann et al. (2009), which reveal a reversal from westerly to easterly flow that initiates at very high altitudes and gradually descends all

the way to the surface over a period of weeks: the fingerprint of descending NAM anomalies associated with the SSW. Remaining panels replace those analyzed winds from 22-28 January with high-altitude forecasts: a control (panel b) and two other forecasts which were perturbed with the leading stratospheric singular vector perturbations, +SV1 and –SV1 (panels c and d, respectively) as shown in Figures 8a-c. The growing +SV1 perturbations to the initial conditions, which take the form of an hemispheric NAM structure, enhance the strength of the SSW, as reflected in Figures 9c in the magnitude of forced stratospheric easterlies and the descent rate of easterly shear zones, leading to mean easterlies in the high-latitude troposphere and stratosphere after 3–4 days. Conversely, −SV1-perturbed forecasts weaken and halt the warming, yielding a minor SSW with mean westerlies throughout the high-latitude troposphere and stratosphere after ~4 days in Figure 9d. This forecast SSW sensitivity to growing ±SV1 perturbations arises as a positive feedback driven by reinforcing changes in planetary-wave Eliassen-Palm (EP) fluxes, with +SV1-perturbed forecasts increasing poleward EP fluxes and −SV1-perturbed forecasts increasing equatorward and decreasing poleward EP fluxes. This work has been written up and submitted to the peer-reviewed scientific literature (Coy et al. 2012).

Tasks R2f. This task awaits further progress on Task R2c.

IMPACT/APPLICATIONS

Naval Meteorology and Oceanography Command (CNMOC) has identified NAVGEM as the Navy's bridge strategy from its current NWP capability (NOGAPS) to a future seamless Earth System Prediction Capability (ESPC) predicting the atmosphere seamlessly across time scales from days to decades. The improved NAVGEM seasonal prediction capabilities provided by this project are moving the Navy closer to a future operational ESPC generating ensemble forecasts on a continuum of time scales spanning weather and climate. Specifically, improved models of deep stratosphere-troposphere coupling provided by this research are improving NAVGEM's ability to predict deeply coupled regional weather events and systems that are highly relevant for day-to-day Navy operations, such as severe Arctic temperature anomalies, gale-force oceanic winds and high ocean-wave conditions that are all affected by deep coupling of NAM/SAM anomalies from the stratosphere to the surface (e.g., Thompson et al. 2002).

TRANSITIONS

We transitioned a series of new code options to the NAVGEM "trunk" and "development" code repositories, including new L50, L64 and L71 layers and initial SSMIS UAS data assimilation code.

RELATED PROJECTS

Doyle, J. D., and S. D. Eckermann, *The Boundary Paradox*, NRL 6.1 Accelerated Research Initiative, 1 October 2010-30 September 2015.

Eckermann, S. D, and collaborators, *New Approaches to the Parameterization of Gravity-Wave and Flow-Blocking Drag due to Unresolved Mesoscale Orography Guided by Mesoscale Model Predictability Research*, ONR Award Number: N0001411WX21220, 1 October 2011-30 September 2014.

Hoppel, K. W., *High Altitude Data Assimilation for NWP*, NRL 6.2 Work Unit, 1 October 2009-September 2013.

REFERENCES

Allen, M., J. Lunine, and Y. Yung (1984), The vertical distribution of ozone in the mesosphere and lower thermosphere, J. Geophys. Res., 89, 4841–4872.

Baldwin, M. P., and T. J. Dunkerton (2001), Stratospheric harbingers of anomalous weather regimes, Science, 244, 581–584.

Baldwin, M.P., D.B. Stephenson, D.W.J. Thompson, T.J. Dunkerton, A.J. Charlton, A. O'Neill (2003), Stratospheric memory and extended-range weather forecasts, Science, 301, 636-640.

Bell, C. J., L. J. Gray, A. J. Charlton-Perez, M. M. Joshi, and A. A. Scaife (2009), Stratospheric communication of El Niño teleconnections to European winter. J. Climate, 22, 4083–4096.

Clough, S. A., M. W. Shephard, E. J. Mlawer, J. S. Delamere, M. J. Iacono, K. Cady-Pereira, S. Boukabara, and P. D. Brown (2005), Atmospheric radiative transfer modeling: A summary of the AER codes: Short communication, J. Quant. Spectrosc. Radiat. Transfer, 91, 233–244.

Coy, L., S. D. Eckermann, K. W. Hoppel, and F. Sassi (2011), Mesospheric precursors to the major stratospheric sudden warming of 2009: Validation and dynamical attribution using a ground-to-edge-of-space data assimilation system, J. Adv. Model. Earth Syst., 3, M10002, 7pp., doi:10.1029/2011MS000067.

Eckermann, S. D., K. W. Hoppel, L. Coy, J. P. McCormack, D. E. Siskind, K. Nielsen, A. Kochenash, M. H. Stevens, C. R. Englert, and M. Hervig (2009), High-altitude data assimilation system experiments for the northern summer mesosphere season of 2007, J. Atmos. Sol.-Terr. Phys., 71, 531-551.

Eckermann, S. D. (2011), Explicitly stochastic parameterization of nonorographic gravity-wave drag, J. Atmos. Sci., 68, 1749-1765.

Eckermann, S. D. and J. P. McCormack (2012), Extension of linearized parameterizations of gas-phase stratospheric ozone photochemistry through the upper stratosphere, mesosphere and lower thermosphere, (paper in preparation).

Han, Y, et al. (2007), A fast radiative transfer model for SSMIS upper atmosphere sounding channels. J. Geophys. Res., 112, D11121, doi:10.1029/2006JD008208.

Han, Y., P. van Delst, and F. Weng (2010), An improved fast radiative transfer model for special sensor microwave imager/sounder upper atmosphere sounding channels. J. Geophys. Res., 115, D15109, doi:10.1029/2010JD013878.

Hoppel, K. W., N. L. Baker, L. Coy, S. D. Eckermann, J. P. McCormack, G. E. Nedoluha, and D. E. Siskind (2008), Assimilation of stratospheric and mesospheric temperatures from MLS and SABER into a global NWP model, Atmos. Chem. Phys., 8, 6103-6116.

Hoppel, K. W., S. D. Eckermann, G. E. Nedoluha, D. R. Allen, S. D. Swadley, N. L. Baker, and L. Coy (2012), Evaluation of SSMIS upper atmosphere sounding channels for high-altitude data assimilation, paper in preparation.

Hurrell, J.W., Y. Kushnir, G. Ottersen, and M. Visbeck (2003), *The North Atlantic Oscillation: Climate Significance and Environmental Impact*, AGU Geographical Monograph Ser. 134, 279pp.

Ineson, S., and A. A. Scaife (2009), The role of the stratosphere in the European climate response to El Niño, Nat. Geosci., 2, 32–36.

McCormack, J. P., S. D. Eckermann, D. E. Siskind, and T. J. McGee (2006), CHEM2D-OPP: A new linearized gas-phase ozone photochemistry parameterization for high-altitude NWP and climate models, Atmos. Chem. Phys., 6, 4943-4972.

Mlawer, E. J., S. J. Taubman, P. D. Brown, M. J. Iacono, and S. A. Clough (1997), Radiative transfer for inhomogeneous atmospheres: RRTM, a validated correlated-k model for the longwave, J. Geophys. Res., 102, 16,663–16,682.

NAS (2010), Assessment of intraseasonal and interannual climate prediction and variability, Committee on Assessment of Intraseasonal to Interannual Climate Prediction and Predictability, National Research Council, The National Academies Press, 192pp (http://www.nap.edu/catalog.php?record_id=12878).

Thompson, D. W. J., M. P. Baldwin, and J. M. Wallace (2002), Stratospheric connection to Northern Hemisphere wintertime weather: Implications for prediction, J. Climate, 15, 1421-1428.

WCRP (2008), Position paper on seasonal prediction, First WCRP Seasonal Prediction Workshop, 4-7 June 2007, Barcelona, Spain, Report No. 3/2008, ICPO Publication No. 127, 23pp.

(http://www.wcrp-climate.org/documents/WCRP_SeasonalPrediction_PositionPaper_Feb2008.pdf).

Weare, B. C., C. Cagnazzo, P. G. Fogli, E. Manzini, and A. Navarra (2012), Madden-Julian Oscillation in a climate model with a well-resolved stratosphere, J. Geophys. Res., 117, D01103, doi:10.1029/2011JD016247.

PUBLICATIONS

Coy, L., C. A. Reynolds, and S. D. Eckermann (2012), Structure and evolution of stratospheric singular vectors during the January 2009 stratospheric sudden warming, Quart. J. Roy. Meteorol. Soc., (submitted August 2012).

Eckermann, S. D. and J. P. McCormack (2012), Extension of linearized parameterizations of gas-phase stratospheric ozone photochemistry through the upper stratosphere, mesosphere and lower thermosphere, (paper in preparation).

Hoppel, K. W., S. D. Eckermann, G. E. Nedoluha, D. R. Allen, S. D. Swadley, N. L. Baker, and L. Coy (2012), Evaluation of SSMIS upper atmosphere sounding channels for high-altitude data assimilation, paper in preparation.